5-1986

# A Predictive-Adaptive, Multipoint Feedback Controller for Local Heat Therapy of Solid Tumors

Charles F. Babbs
*Purdue University*, babbs@purdue.edu

V A. Vanguine

J T. Jones

# A Predictive-Adaptive, Multipoint Feedback Controller for Local Heat Therapy of Solid Tumors

C. F. BABBS[1], V. A. VAGUINE[2], AND J. T. JONES[1]

1. Biomedical Engineering Center, Purdue University, West Lafayette, Indiana 47907, USA.
2. Clini-Therm Corporation, Dallas, TX 75243, USA

**Abstract**—Uniform heating of tumor tissue to therapeutic temperatures without damaging surrounding normal tissue is required for optimal local heat therapy of cancer. This paper describes an algorithm for online computer control that will allow the therapist to minimize the standard deviation of measured intratumoral temperatures. The method is applicable to systems incorporating multiple surface and/or interstitial applicators delivering microwave, radiofrequency, or ultrasonic power and operating under the control of a small computer. The essential element is a novel predictive-adaptive control algorithm that infers relevant thermal parameters from the responses of multiple temperature sensors, as each of the power applicators is briefly turned off. Applied power and effective perfusion are estimated from transient slope changes of the temperature-time curves for each sensor. By substituting these values into a system of linear equations derived from the bio-heat transfer equation, the small computer can calculate the optimal allocation of power among the various applicators ("knob settings") to generate most uniform intratumoral temperature distribution with the desired mean, or minimum, tumor temperature.

**Key words:** Hyperthermia, computer control, treatment planning, multipoint feedback control.

NOMENCLATURE

Subscripts

$i = 1, 2, 3,. k$     denote external or interstitial applicators, each at a fixed position in space.

$j = 1, 2, 3,..n$     denote points in the tumor at which temperature, applied power density, and effective perfusion are measured and for which predicted temperatures are calculated.

Fundamental Variables

$P'_{i,j}$     estimated power density (SAR) that would be generated at point j, assuming all power is delivered via applicator i.

$\sigma_i$     fraction of total power delivered through applicator.

$P'_j$     net predicted power at point j from all applicators $= \sum_{i=1}^{k} \sigma_i P'_j$.

$\omega'_j$     apparent perfusion (SCR) at point j calculated from thermal washout.

$\Delta t$     diagnostic cycle time.

$\Delta T_j$     temperature rise at point j.

Derived Variables

$\Delta T_j^0$     temperature rise above arterial temperature at measuring point j at beginning of next diagnostic cycle = end of current diagnostic cycle.

$\alpha_j$     $= 0.5\omega'_j c_b \Delta t /(\rho c)$, a dimensionless dummy variable related to heat loss during the diagnostic cycle.

$d_{i,j}$     $= \left(\Delta t /(\rho c) P_{i,j}\right)/(1+\alpha_j)$, a dummy variable with units of temperature.

$\overline{\Delta T}$     mean predicted temperature rise for all measuring points 1 to n.

$\Delta T^{0'}$     mean initial temperature rise for all measuring points 1 to n at beginning of next diagnostic cycle.

$\bar{d}_i$      mean value of $d_{i,j}$ for all points $j = 1$ to $n$, a dummy variable associated with each applicator.

r      power multiplier; total power required to achieve target temperature at end of next diagnostic cycle divided by total power of current diagnostic cycle.

## I. INTRODUCTION

During local heat therapy for a circumscribed tumor mass, the therapist strives to elevate intratumoral temperature uniformly to a therapeutic, tumor killing level while maintaining surrounding normal tissue at a safe, nonlethal temperature. In the ideal limiting case, the temperature distribution in space would approach a step function, abruptly rising to a constant therapeutic level at the tumor edge (Fig. 1). It is useful to describe such an ideal temperature distribution as having two essential properties:

(1)      A clear separation of the mean intratumoral temperature from the mean temperature of surrounding normal tissue during treatment.

(2)      Minimum spatial variation in intratumoral temperatures.

The first property describes selectivity of heating; the second property describes uniformity of heating.

An effective biological means for enhancing the selectivity of local heat treatment is through the use of vasodilator drugs, which favorably alter the partitioning of blood flow between tumor and surrounding normal tissue [1]-[3]. Complementary technological means of enhancing selectivity include schemes for focusing power deposition within the tumor mass, such as multiple ultrasonic beams or interstitial microwave antennas [4]-[6].

**TUMOR**                 **NORMAL TISSUE**

IDEAL
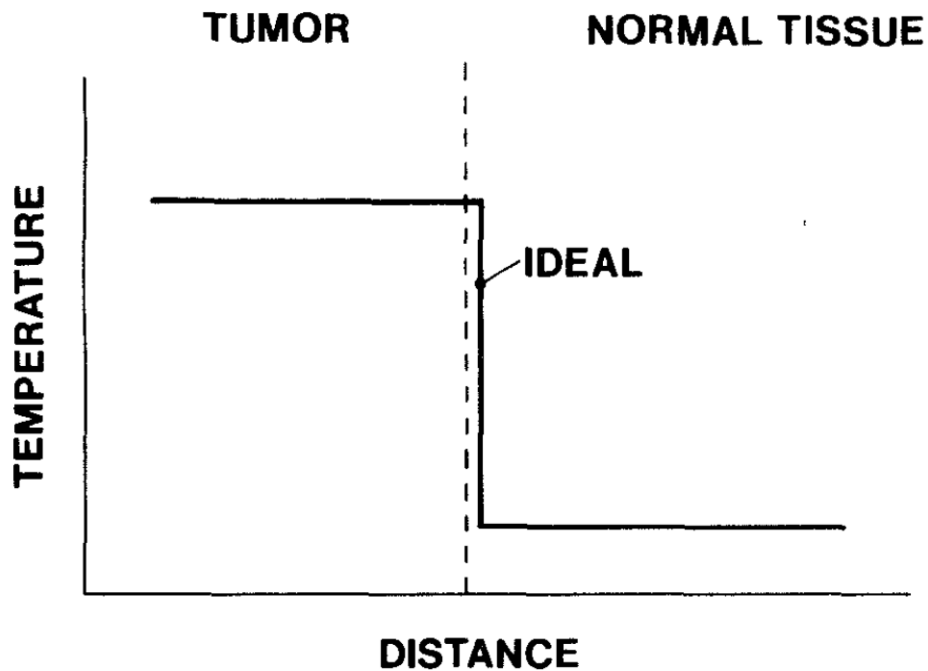
**TEMPERATURE**

**DISTANCE**

Fig. 1. Concept of ideal local heat therapy for a circumscribed lesion. Tumor temperature is uniformly elevated with respect to surrounding normal tissue. The variability of intratumoral temperatures is nil.

There remains, however, the problem of achieving maximal uniformity of tumor temperatures. Some method is needed to adjust power in the multiple applicators to avoid treatment failures associated with cold spots in the tumor, as well as possible complications associated with hot spots within the treatment field. The present paper describes a predictive-adaptive control algorithm that enhances the uniformity of intratumoral temperature distributions by favorably adjusting and continually readjusting the proportion of power applied to various surface and/or interstitial applicators during the course of a treatment session.

II. COMPUTATIONAL METHODS

The computational approach we present for predictive-adaptive, multipoint feedback control of multi-applicator hyperthermia systems has three major aspects. The first is the means by which a microcomputer can estimate applied power density and "effective perfusion" from temperature data recorded from each of several temperature probes embedded in the tissue. The second is the means by which the computer can repeatedly calculate the optimal partitioning of total power among the various applicators by solving a set of simultaneous, linear equations. The third is the means by which total power is then scaled to achieve the desired mean (or minimum) intratumoral temperature.

4

A. Real-Time Estimation of Thermal Parameters

Previous reports have described the well-known technique in which, assuming that initial tissue temperature is stable and equal to arterial blood temperature, specific absorption rate (SAR) of applied energy (i.e., power) can be estimated from the slope of the temperature-time curve during a brief period of heating, according to the expression

$$SAR = \rho c \frac{dT}{dt}$$

where $\rho$ is tissue density, $c$ is tissue specific heat, $T$ is temperature, and $t$ is time [1], [7]. It is equally true, however, from inspection of the bio-heat equation, that if at any time during tissue heating power is suddenly turned off, the SAR just prior to turn-off must be equal to the resultant slope change, i.e.,

$$SAR = \left( \rho c \frac{dT}{dt} \right)_{before} - \left( \rho c \frac{dT}{dt} \right)_{after}.$$

A hyperthermia treatment usually lasts 30 to 60 min. The time required to monitor slope changes after power-off is roughly 30 sec, an interval typically short with respect to thermal time constants in tissue. The specific contribution of each applicator to the net SAR can be obtained by analysis of the effect upon temperature at each monitored location caused by turning the power to the applicator off for about 30 sec. In a similar way, "effective perfusion" or "specific cooling rate" (SCR) can be determined from the slope of the temperature-time curves at each monitored site when all power is briefly turned off, using the expression

$$SCR = -\frac{\rho c}{c_b \Delta T} \frac{d(\Delta T)}{dt}$$

where $c_b$ is the blood specific heat and $\Delta T$ is the tissue temperature rise above arterial temperature. We refer to the process of measuring the power contribution of each applicator and the effective perfusion at each site as a diagnostic cycle. Since the distribution of perfusion (typically the dominant component of SCR) in adjacent normal tissues changes during the hyperthermia treatment, and since power will be deliberately changed under computer control, it is necessary to repeat the diagnostic cycle continually to obtain updated values. In this way, the essential heat transfer parameters for predictive control of the temperature distribution can be monitored by simple manipulation of input power under computer control.

B. Computation of Power Fractionation for Minimal Standard Deviation of Measured Intratumoral Temperatures

The mathematical approach we propose for computation of the optimal power fractionation from the set of estimated SAR and SCR data at each monitored intratumoral site is based upon the concept that the net SAR from multiple applicators is a linear combination of the contributions to SAR generated by the individual applicators, which are in turn proportional to the fraction, σ, of the total power allocated to each. That is, we assume an incoherent mode of incident power, in which effects of phase addition and cancellation can be ignored. It is possible, then, to write an expression for the variance of the intratumoral temperatures (mean squared deviation about the mean temperature) as a function of the u values. We wish to know the rr values that minimize this variance. By differentiating the expression for the variance with respect to each u value and setting the partial derivatives equal to zero, we shall obtain a set of simultaneous linear equations that can be solved for the unique set of σ values giving minimum intratumoral temperature variation. The derivation is as follows.

Consider, in particular, a situation in which a tumor is heated by k different applicators arranged in and around the tumor mass, as sketched in Fig. 2. Let the relevant variables be defined as indicated in the Nomenclature.
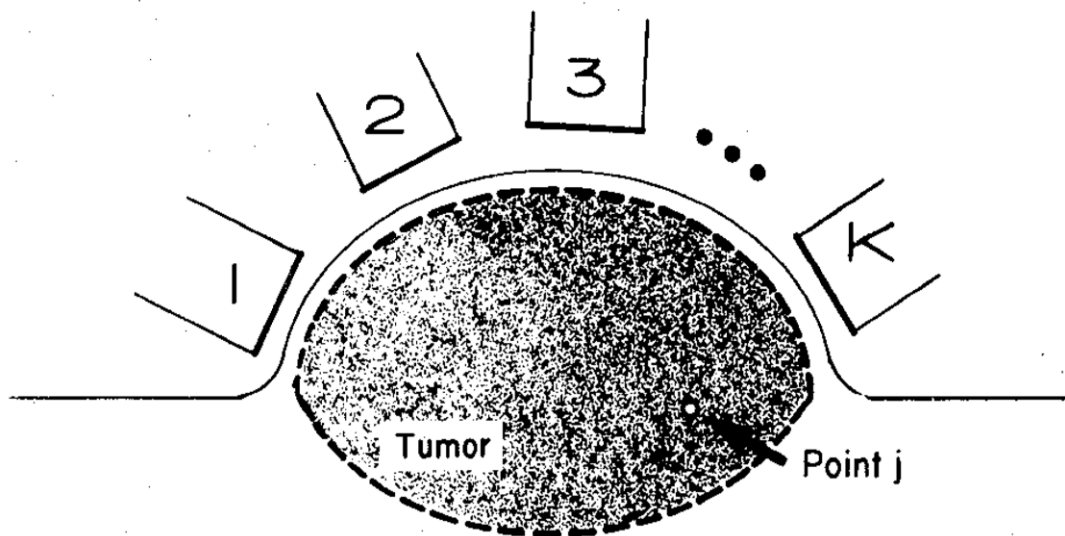


Fig. 2. General scheme of multi-applicator hyperthermia treatment assumed in derivation. The derivation is valid for interstitial as well as the external applicators shown,

The rationale for optimal power partitioning is as follows. The net power at point j is

$$P_j = \sigma_1 P_{1j} + \sigma_2 P_{2j} + \cdots + \sigma_k P_{kj}$$

where

$$\sigma_1 + \sigma_2 + \cdots + \sigma_k = 1.$$

Here the first subscript of P represents an applicator from 1 to k and the second subscript of P represents a point of intratumoral temperature measurement from 1 to n. Recall that $P_{i,j}$ represents the SAR at point j if 100 percent of the applied power were delivered continuously via applicator, i. It is obtained from the change in slope of the temperature time function at point j as power to applicator i is briefly interrupted, divided by the current value of $\sigma_i$. Now consider a marching solution to the bio-heat equation at point j as

$$P_j - w_j' c_b \Delta T = \rho c \frac{d(\Delta T_j)}{dt}$$

where $\Delta T$ = temperature rise above arterial temperature. Letting $\Delta T^0$ represent the current temperature rise, we can estimate the temperature rise at point j after a small time step, dt, as

$$\Delta T_j = \Delta T_j^0 + \frac{dt}{\rho c} \left( \sigma_1 P_{1j}' + \sigma_2 P_{2j}' + \cdots \right.$$
$$\left. + \sigma_k P_{kj}' - w_j' c_b \Delta T_j^0 \right).$$

If power is applied throughout the next diagnostic cycle for m such small time steps in succession

$$\Delta T_j = \Delta T_j^0 + m \frac{dt}{\rho c} \left( \sigma_1 P_{1j}' + \sigma_2 P_{2j}' + \cdots + \sigma_k P_{kj}' \right)$$
$$- \frac{w_j' c_b}{\rho c} \sum_{p=0}^{m} \Delta T_j^p \, dt.$$

Passing to the integral as a representation of the sum, and using the trapezoidal rule to approximate the integral, we have

$$\sum_{p=0}^{m} \Delta T_j^p \, dt = 0.5 \left( \Delta T_j^0 + \Delta T_j \right) m \, dt$$

and after m steps

$$\Delta T_j = \Delta T_j^0 + m \frac{dt}{\rho c} \left( \sigma_1 P'_{1j} + \sigma_2 P'_{2j} + \cdots + \sigma_k P'_{kj} \right)$$
$$- \frac{w'_j c_b}{2 \rho c} \left( \Delta T_j^0 + \Delta T_j \right) m \, dt.$$

Now substituting the cycle time $\Delta t = m\, dt$, and solving for the temperature rise $\Delta T_j$ at the end of the next diagnostic cycle

$$\Delta T_j = \Delta T_j^0 \frac{1 - \alpha_j}{1 + \alpha_j} + \frac{\Delta t}{\rho c} \left( \sigma_1 P'_{1j} + \sigma_2 P'_{2j} \right.$$
$$\left. + \cdots + \sigma_k P'_{kj} \right) \frac{1}{1 + \alpha_j}$$

where

$$\alpha_j = \frac{w'_j c_b \Delta t}{2 \rho c}$$

is a dimensionless indicator of effective perfusion. Now, for simplicity, letting the doubly subscripted dummy variable

$$d_{ij} = \frac{\Delta t}{2 \rho c} \frac{P'_{ij}}{1 + \alpha_j}$$

and letting

$$\Delta T_j^{0'} = \Delta T_j^0 \frac{1 - \alpha_j}{1 + \alpha_j}$$

we have

$$\Delta T_j = \Delta T_j^{0'} + \sigma_1 d_{1j} + \sigma_2 d_{2j} + \cdots + \sigma_k d_{kj}.$$

8

This is an expression for estimated temperature at the end of the next diagnostic cycle as a function of the prevailing applied power, effective perfusion, and partitioning of applied power according to the $\sigma$ values. We seek to pick the $\sigma$ values such that the sum

$$S = \sum_{j=1}^{n} \left( \Delta T_j - \overline{\Delta T} \right)^2$$

for points 1 to n within the tumor is minimized, i.e., to choose the $\sigma$ values for most uniform heating. Because their sum must equal 1, only $k - 1$ of the $\sigma$ values may be specified independently.

So let us write $\Delta T_j$ and $\overline{\Delta T}$ in terms of the first $k - 1$ values of $\sigma$, taking

$$\sigma_k = 1 - (\sigma_1 + \sigma_2 + \cdots + \sigma_{k-1}).$$

Thus

$$
\begin{aligned}
\Delta T_j &= \Delta T_j^{0'} + \sigma_1 d_{1j} + \sigma_2 d_{2j} + \cdots + \sigma_{k-1} d_{k-1,j} \\
&\quad + (1 - \sigma_1 - \sigma_2 - \cdots - \sigma_{k-1}) d_{kj} \\
&= \Delta T_j^{0'} + d_{kj} + \sigma_1 (d_{1j} - d_{kj}) + \sigma_2 (d_{2j} - d_{kj}) \\
&\quad + \cdots + \sigma_{k-1,j} (d_{k-1,j} - d_{kj})
\end{aligned}
$$

and

$$
\begin{aligned}
\overline{\Delta T} &= \frac{1}{n} \sum_{j=1}^{n} \Delta T_j \\
&= \Delta \overline{T}^{0'} + \bar{d}_k + \sigma_1 (\bar{d}_1 - \bar{d}_k) + \sigma_2 (\bar{d}_2 - \bar{d}_k) \\
&\quad + \cdots + \sigma_{k-1} (\bar{d}_{k-1} - \bar{d}_k).
\end{aligned}
$$

Now, the $\sigma$ values for minimum S will be found from the solution of the $k - 1$ simultaneous, normal equations

$$\frac{dS}{d\sigma_1} = 0, \quad \frac{dS}{d\sigma_2} = 0, \cdots, \quad \frac{dS}{d\sigma_{k-1}} = 0$$

for the $k - 1$ unknown $\sigma$ values, where the i-th such equation is

9

$$\frac{dS}{d\sigma_i} = \sum_{j=1}^{n} 2\left(\Delta T_j - \overline{\Delta T}\right) \frac{d}{d\sigma_i}\left(\Delta T_j - \overline{\Delta T}\right).$$

Substituting for $\Delta T_j$ and $\overline{\Delta T}$, we have the i-th equation in the set

$$\begin{aligned}
\frac{dS}{d\sigma_i} = &\sum_{j=1}^{n} 2\sigma_1\left(d_{1j} - d_{kj} - (\bar{d}_1 - \bar{d}_k)\right) \\
&\times \left(d_{ij} - d_{kj} - (\bar{d}_i - \bar{d}_k)\right) \\
&+ \sum_{j=1}^{n} 2\sigma_2\left(d_{2j} - d_{kj} - (\bar{d}_2 - \bar{d}_k)\right) \\
&\times \left(d_{ij} - d_{kj} - (\bar{d}_i - \bar{d}_k)\right) + \cdots \\
&+ \sum_{j=1}^{n} 2\sigma_{k-1}\left(d_{k-1} - d_{kj} - (\bar{d}_{k-1} - \bar{d}_k)\right) \\
&\times \left(d_{ij} - d_{kj} - (\bar{d}_i - \bar{d}_k)\right) \\
&+ \sum_{j=1}^{n} \left(\Delta T_j^{0'} - \overline{\Delta T}^{0'} + d_{kj} - \bar{d}_k\right) \\
&\times \left(d_{ij} - d_{kj} - (\bar{d}_i - \bar{d}_k)\right).
\end{aligned}$$

Now dividing through by two, setting $dS/\sigma_i = 0$, and factoring out the $\sigma$ terms, we have the i-th equation

$$0 = \sigma_1 \sum_{j=1}^{n} \left( d_{1j} - \bar{d}_1 - \left( d_{kj} - \bar{d}_k \right) \right)$$

$$\times \left( d_{ij} - \bar{d}_i - \left( d_{kj} - \bar{d}_k \right) \right)$$

$$+ \sigma_2 \sum_{j=1}^{n} \left( d_{2j} - \bar{d}_2 - \left( d_{kj} - \bar{d}_k \right) \right)$$

$$\times \left( d_{ij} - \bar{d}_i - \left( d_{kj} - \bar{d}_k \right) \right) + \cdots$$

$$+ \sigma_{k-1} \sum_{j=1}^{n} \left( d_{k-1,j} - \bar{d}_{k-1} - \left( d_{kj} - \bar{d}_k \right) \right)$$

$$\times \left( d_{ij} - \bar{d}_i - \left( d_{kj} - \bar{d}_k \right) \right)$$

$$+ \sum_{j=1}^{n} \left( \Delta T_j^{0'} - \overline{\Delta T}^{0'} + d_{kj} - \bar{d}_k \right)$$

$$\times \left( d_{ij} - \bar{d}_i - \left( d_{kj} - \bar{d}_k \right) \right).$$

There are $k - 1$ such equations and $k - 1$ unknown o values corresponding to the indices $i = 1$ to $k - 1$. This terminology can be simplified by writing the above as

$$\sigma_1 \sum_{j=1}^{n} a_{1j} a_{ij} + \sigma_2 \sum_{j=1}^{n} a_{2j} a_{ij} + \cdots$$

$$+ \sigma_{k-1} \sum_{j=1}^{n} a_{k-1,j} a_{ij}$$

$$= - \sum_{j=1}^{n} \left( \Delta T_j^{0'} - \overline{\Delta T}^{0'} + \left( d_{kj} - \bar{d}_k \right) \right) a_{ij}$$

for the i-th equation in the series, where

$$a_{ij} \equiv d_{ij} - \bar{d}_i - \left( d_{kj} - \bar{d}_k \right)$$

with $i$ referring to the applicator number and $j$ referring to the point number. The entire set of $i$ equations is then rendered as

$$\sigma_1 \sum_{j=1}^{n} a_{1j}^2 + \sigma_2 \sum_{j=1}^{n} a_{2j} a_{1j} + \cdots$$

$$+ \sigma_{k-1} \sum_{j=1}^{n} a_{k-1,j} a_{1j}$$

$$= - \sum_{j=1}^{n} \left( \Delta T_j^{0\prime} - \overline{\Delta T}^{0\prime} + d_{kj} - \bar{d}_k \right) a_{1j}$$

$$\sigma_1 \sum_{j=1}^{n} a_{1j} a_{2j} + \sigma_2 \sum_{j=1}^{n} a_{2j}^2 + \cdots$$

$$+ \sigma_{k-1} \sum_{j=1}^{n} a_{k-1,j} a_{2j}$$

$$= - \sum_{j=1}^{n} \left( \Delta T_j^{0\prime} - \overline{\Delta T}^{0\prime} + d_{kj} - \bar{d}_k \right) a_{2j}$$

$$\cdots$$
$$\cdots$$
$$\cdots$$

$$\sigma_1 \sum_{j=1}^{n} a_{1j} a_{k-1,j} + \sigma_2 \sum_{j=1}^{n} a_{2j} a_{k-1,j} + \cdots$$

$$+ \sigma_{k-1} \sum_{j=1}^{n} a_{k-1,j}^2$$

$$= - \sum_{j=1}^{n} \left( \Delta T_j^{0\prime} - \overline{\Delta T}^{0\prime} + d_{kj} - \bar{d}_k \right) a_{k-1,j}.$$

This set of equations is easily solved by numerical methods. The coefficients of the $\sigma$ terms are

$$C_{pq} = \sum_{j=1}^{n} a_{qj} a_{pj} \qquad \text{for equation } p, \text{column } q.$$

The solution of these linear equations defining the optimal $\sigma$ values can be easily done by a commercial microcomputer in conjunction with software that computes and stores SAR and SCR values. Such a task, as opposed to tasks requiring clinical judgment and knowledge of anatomy and patient geometry, is appropriately accomplished by a digital computer.

C. Computation of Optimal Total Power

Knowing the optimal set of $\sigma$ values, it is then straightforward to compute the recommended total applied power required to achieve a user-specified mean or minimal target temperature. This may be done by several methods. A simple and effective strategy that takes advantage of knowledge of thermal parameters is as follows. Suppose that we find the $\sigma$ values for minimal standard deviation using the current value of total applied power. The mean estimated temperature rise, $\overline{\Delta T}$, at the end of the next diagnostic cycle is

$$\overline{\Delta T} = \frac{1}{n} \sum_{j=1}^{n} \left( \Delta T_j^{0'} + \sigma_1 d_{1j} + \sigma_2 d_{2j} + \cdots + \sigma_k d_{kj} \right)$$

where

$$d_{1j} = \frac{\Delta t}{2\rho c} \frac{P'_{1j}}{1 + \alpha_j}$$

as before.

If the new total power is $r$ times the current power, partitioned according to the previously determined $\sigma$ values, then after power adjustment

$$\overline{\Delta T} = \frac{1}{n} \sum_{j=1}^{n} \left( \Delta T_j^{0'} + \sigma_1 r d_{1j} + \sigma_2 r d_{2j} + \cdots + \sigma_k r d_{kj} \right)$$

$$= \overline{\Delta T}^{0'} + r \left( \sigma_1 \bar{d}_1 + \sigma_2 \bar{d}_2 + \cdots + \sigma_k \bar{d}_k \right).$$

Setting $\overline{\Delta T}$ equal to the target temperature rise, we can solve for the power multiplier required as

$$r = \frac{\text{target} - \overline{\Delta T}^{0'}}{\sigma_1 \bar{d}_1 + \sigma_2 \bar{d}_2 + \cdots + \sigma_k \bar{d}_k}.$$

Thus, we can select the value of $r$ to give the desired mean temperature at the end of the next diagnostic cycle, which at the same time has minimal standard deviation. The applied power levels or "control knob settings" for each applicator are then multiplied by $(\sigma_{\text{new}} - \sigma_{\text{old}})$ r to

obtain the revised power settings predicted to generate a measured intratumoral temperature distribution that has both minimal standard deviation and on-target mean temperature. If the therapist prefers to define the target in terms of the minimal sensed intratumoral temperature, then a similar process can be followed, in which the smallest predicted tumor temperature at the end of the next diagnostic cycle is substituted for mean temperature.

## III. SIMULATIONS OF CONTROLLER PERFORMANCE

We have simulated this proposed control procedure on a mainframe computer, using one program that solves a one-dimensional version of the bio-heat equation [8] to simulate temperature changes in tissue and another program that implements the online control algorithm. Although compiled together, the two programs are logically independent, so that a real thermometry system and patient or phantom can be substituted for the bio-heat equation model with only trivial changes to the control software.

A simplified version of the control algorithm is presented in Fig. 3. The program first reads treatment specifications from a disk file, including such information as the target temperature, the number of power applicators, and the location of temperature probes (whether in tumor or normal tissue). Initial conditions of the thermal model are then read from a separate file. Then the control program loops through diagnostic and power update cycles, as long as the prescribed treatment time has not elapsed. During a diagnostic cycle, power to each of the multiple applicators is sequentially turned off for a brief period (e.g., 20 sec). The contribution of each applicator to net SAR and the effective perfusion at each monitored site are then computed from slope changes.

In the current implementation, the slope change at a given monitoring site that would occur when all applicators are turned off is estimated from the sum of slope changes that occur when each applicator is turned off separately. This feature shortens the diagnostic cycle and eliminates large dips in temperature associated with total power-off for many configurations.

The computer then calculates the set of $\sigma$ values, defining the unique partitioning of the current total power that minimizes the standard deviation of predicted intratumoral temperatures at the end of the next diagnostic cycle. The result is a set of revised "knob settings" that indicate new values of power to be applied to each applicator.

Next, the control program computes the scale factor, r, required for mean (or if desired, minimum) intratumoral temperature to equal the target. After a safety check to make sure the revised knob settings are not excessive, the control software closes the loop by adjusting power of the modeled applicators to the new knob settings, writes diagnostic information to a record file, and then, if treatment time is not over, begins another diagnostic cycle.

```
                CONTROL ALGORITHM

read treatment specifications

while (time remains) {

    turn on all applicators, then

    for (all applicators) {
        turn each applicator off, then on
        calculate SAR's from slope changes
    }

    calculate effective perfusion from slopes

    solve equations for optimal partitioning of
    power among the applicators

    estimate mean tumor temperature at end of next
    cycle with new power partitioning and current
    total power

    scale total power so that estimated mean tumor
    temperature equals target temperature
}
```

Fig. 3. Simplified version of the control algorithm. For explanation, see text.


First we tested how the system works in simulation for a simple example, in which the correct solution is intuitively obvious. In this case, two applicators deposit power uniformly in two bands of tumor tissue located at different depths far from the skin surface. One temperature sensor is located in the middle of each band (Fig. 4). Blood flow to the tissue is uniform and constant. Because slope-taking algorithms are known to be sensitive to noise, we added a subroutine to the bio-heat equation model to generate random noise ($\leq 0.05\ ^{\circ}\text{C}$) and then round off temperatures to the nearest $0.1\ ^{\circ}\text{C}$ as a provocative test of the control algorithm. Such noise and round off are typical in commercial thermometry systems used with clinical hyperthermia systems.

COMPUTATIONAL TEST:
BIO HEAT EQUATION MODEL



SAR BAND A          SAR BAND B
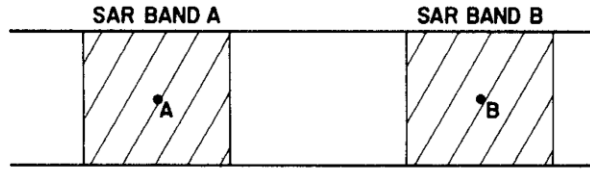
Known Solution: $T_A \simeq T_B$ ; $SAR_A \simeq SAR_B$
Start with $SAR_A = 3\ SAR_B$
Will Algorithm Equalize Temps?

Fig. 4. Sketch of the computational model used in initial tests of algorithm performance. Two bands of tissue are uniformly irradiated. One temperature sensor is located in the middle of each band. Bands are 3.0 cm wide and separated by 3.0 cm in the calculations.
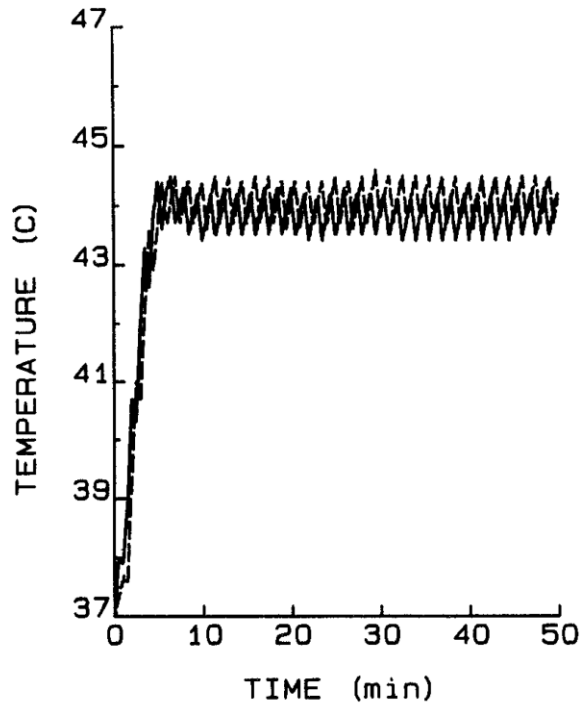


Fig 5, The performance of a control algorithm in simulation, Blood flow is uniform and constant: 200 ml/min/kg. Initial power partitioning was 150 W/kg to band A (solid line) and 50 W/kg to band B (dashed line) The power-off interval was 30 sec. Temperatures were sampled every 2 sec. Optimal solution requires that the two temperatures are equal to each other and equal to the target, here 44 °C. Steady-state portioning of power was 49.9 percent in band A and 50.1 percent in band B.

16

For this simple case, the optimal solution is one in which power is equally partitioned between the two bands so that the temperature at each sensor is on-target and the standard deviation of measured temperatures is zero, i.e., the two temperatures are equal to each other and equal to the target temperature, here 44 $^{\circ}$C. The simulation shown in Fig. 5 was begun with unequal powers, as indicated by the initial slopes: 75 percent (150 W/kg) to band A and 25 percent (50 W/kg) to band B. After the first diagnostic cycle, the system adjusts power to both applicators and the temperatures head toward the target. After two diagnostic cycles, the temperatures settle very near the target. The percentage of total applied power in each band then fluctuates between 49 and 51 percent, very near the correct solution. For comparison, Fig. 6 presents temperature-time curves for exactly the same situation with the control algorithm turned off. Note that steady-state temperatures are widely off-target. The simulated noise and round off of the temperature data are evident.
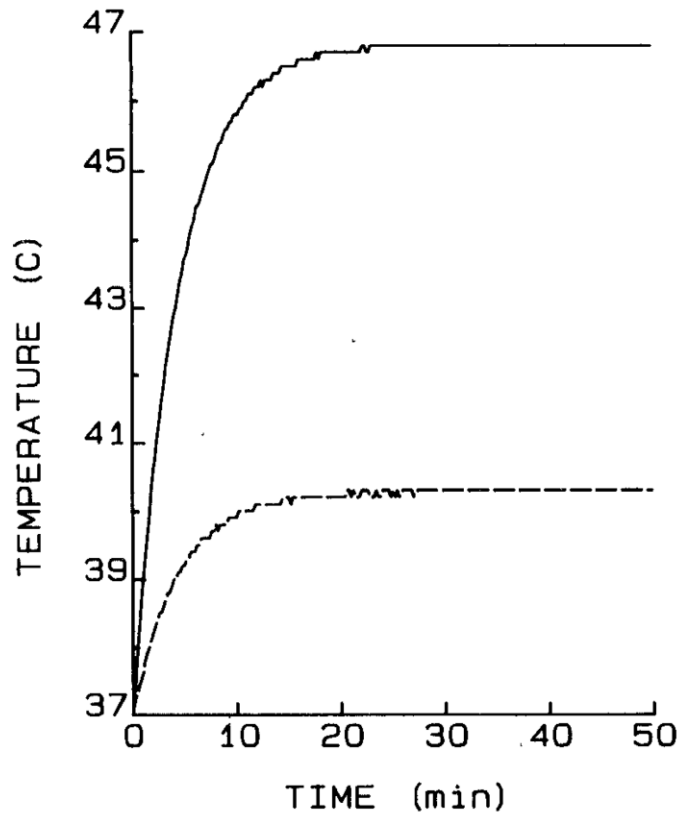


Fig. 6. Control simulation for Fig. 5. Conditions identical to Fig. 5 with the control algorithm turned off. Deliberately introduced noise in the temperature data is evident. The vertical sale identical to that in Fig. 5.
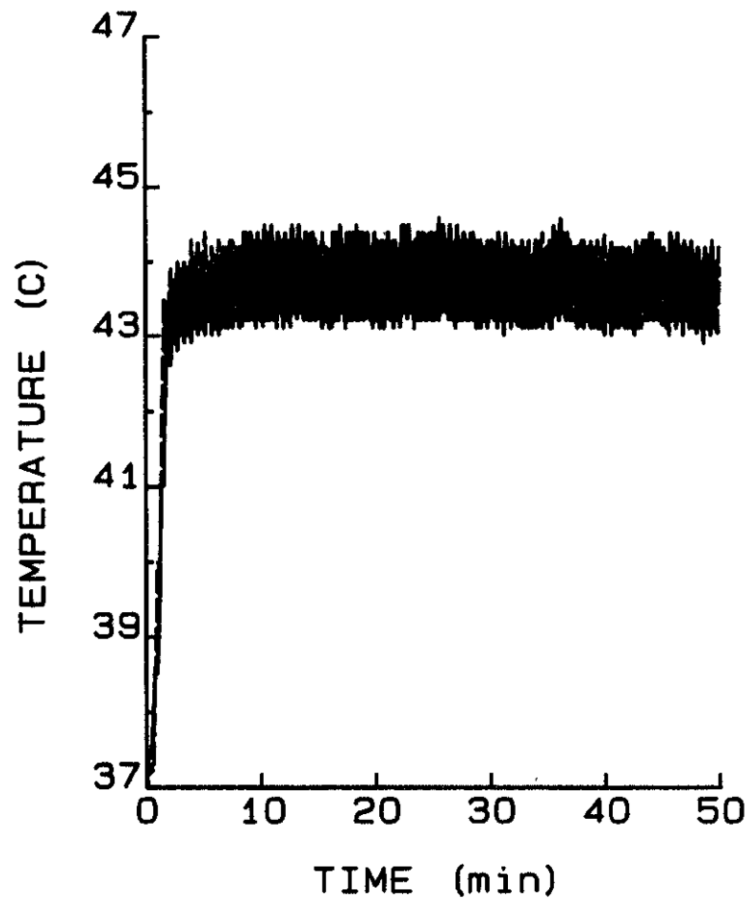
Fig. 7. Algorithm performance with temperature dependent augmentation of blood flow. In this simulation, the thermal model updated perfusion as a function of temperature in a linear fashion up to six-fold over the temperature range from 41 to 46 $^o$C. The power-off interval was 12 sec. Temperatures were sampled every 2 sec. Despite increased perfusion, the algorithm is able to encourage tissue temperatures toward the target level of 44 $^o$C. Solid line = band A; dashed line = band B. Steady-state partitioning of power was 48.4 percent in band A, 51.6 percent in band B.

***Performance with Variable Blood Flow:*** In the previous example, blood flow to the tissue was kept constant. To illustrate the performance of the control algorithm in the presence of changing blood flow, Fig. 7 is presented. Now the thermal model updates tissue perfusion as a function of temperature according to a simplified linear approximation to Song's results [9], [10]: a six-fold increase in blood flow over the temperature range from 41 to 46 $^o$C. Note that despite increased perfusion, the algorithm is able to encourage tissue temperatures toward the target level of 44 $^o$C. In Fig. 8, the same simulation is repeated with the control algorithm disabled. The temperatures are divergent and below the target level.
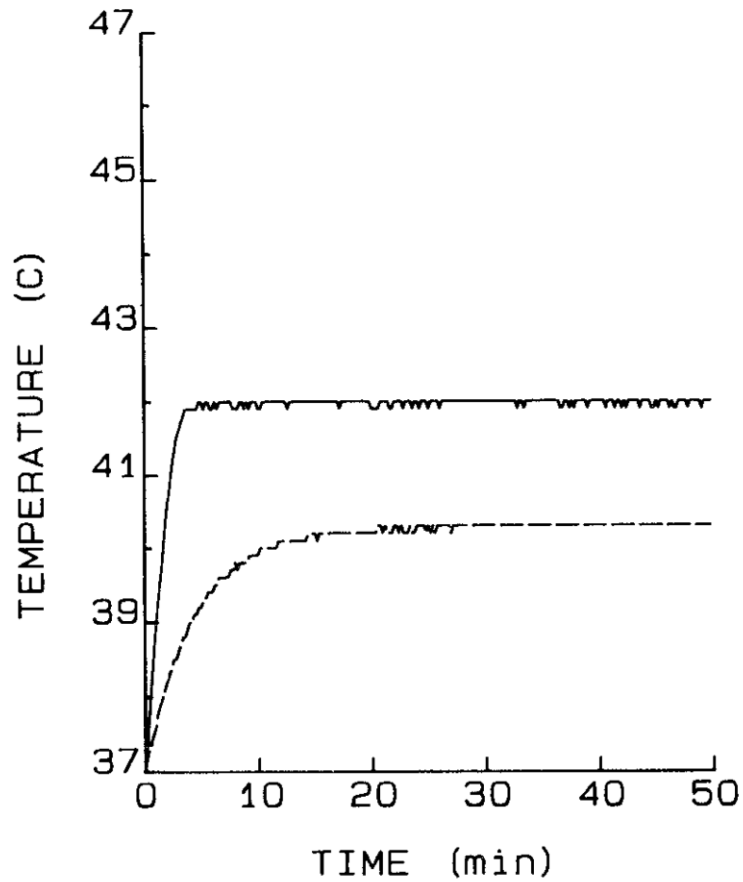
18

Fig. 8. Control simulation for Fig 7. Conditions identical to Fig. 7 with the control algorithm turned off. The temperatures are divergent and off-target. Deliberately introduced noise is evident.

These preliminary results with a one-dimensional computational model of heated tissue serve to illustrate the satisfactory performance of the algorithm in the presence of noise, round-off errors, and variable blood flow. They give us encouragement to pursue development and elaboration of the system in three dimensional computer models and in tests with living normal and tumor tissues.

19

## IV. DISCUSSION

A major improvement in hyperthermia can be expected if spatial temperature distributions could be achieved similar to that depicted in Fig. 1: The present approach implements an algorithm to minimize the standard deviation of measured intratumoral temperatures, and in turn, to adjust total applied power so that the measured tumor temperature distribution is both on-target and maximally uniform.
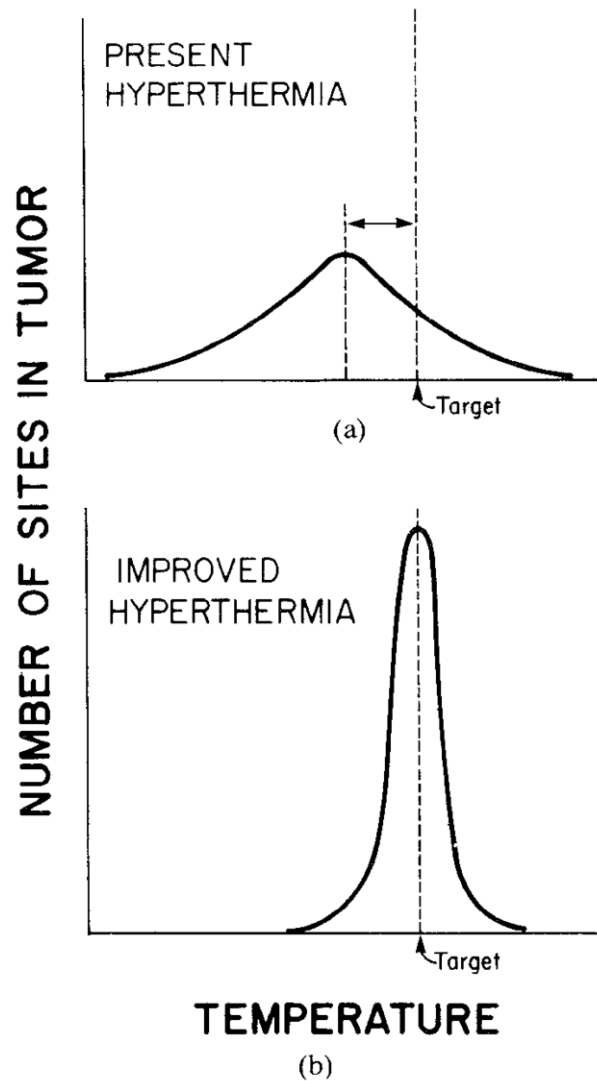


Fig. 9. Concept of present versus improved hyperthermia illustrated with histograms. Wide variation in intratumoral temperatures leads to hot spots and cold spots (a). In an attempt to minimize complications associated with hot spots, total power is limited such that mean temperature is less than the target temperature. In improved hyperthermia with multipoint feedback control, the standard deviation of intratumoral temperatures is reduced, and mean temperature is on target (b).

Dewhirst, Sire, and coworkers have shown a strong correlation between high variability in intratumoral temperature and poor outcome of clinical hyperthermia treatment of spontaneous cancers in pet animals [11]. In essence, they found that if the distribution of temperatures within a tumor shows significant dispersion about its mean value, treatment failures and complications are likely to result. Cold spots never reach therapeutic temperatures, and so are never treated. Hot spots lead to complications such as intolerable pain or ulceration of overlying skin. To avoid complications of hot spots, the therapist is obliged to reduce total applied power, and as a result, mean tumor temperature is often below target (Fig. 9(a)).

The predictive-adaptive control algorithm described in this paper can make for more uniform tumor heating, correct for heat-induced changes in blood flow, and permit improved heat therapy without the moment-to-moment attendance of a physicist, once applicators and temperature sensors have been correctly placed and the treatment started. Because its implementation is substantially dependent upon software rather than hardware, the proposed control scheme can provide great marginal benefit at little marginal cost. Treatment planning is done automatically under computer control during the course of actual therapy. Changes in blood flow due to heat-induced vasodilation in normal tissues, shunting of flow from tumor to normal tissues, and perfusion changes due to thermal damage to capillaries and/or microvascular coagulation are accounted for on a moment-to-moment basis. Formulation of such a dynamic treatment plan lends itself to computer assistance and control since computer based systems can easily conduct regular moment-to-moment monitoring of thermal data as well as rapid analysis, calculation, and adjustment of input power levels.

It is important to point out at this juncture that the system just demonstrated is fundamentally more sophisticated than one in which total power is servo-controlled to maintain the temperature of a single sensor at a target level. This latter type of system is quite inadequate for solving the uniformity problem. Although temperature at a single point in the tumor may be reliably kept on target, there is no guarantee that cold spots do not exist elsewhere in the tumor, and in particular, no guarantee that edge temperatures will be sufficient. Our system optimizes not a single temperature, but the entire sensed temperature distribution. Although more complex than classical controllers, the present algorithm does not require estimation of the entire three dimensional temperature distribution. Rather, the controller deals only with temperatures at measured sites.

Computation time is much less than is required to solve a finite element model: in our experience to date, a few seconds when performed on an IBM-PC. In principle, it should not be necessary for the therapist to enter a description of the geometry, location, and extent of the tumor and surrounding normal tissues, only to identify temperature sensors as being in normal or tumor tissue. Multipoint thermometry and multiple applicators are required, however, and the greater the number of each, the more ideal the control is likely to be. The present approach relies upon the judgment of the therapist about the most reasonable number and placement of temperature probes for sampling of tumor temperature within clinical constraints. We believe that this will prove to be a cost-effective and appropriate mix of art and technology in the practical, clinical setting.

A potential limitation of the present algorithm is that it does require that the multiplexed power sources are non-interfering. For certain microwave systems, the assumption of linear combination of SAR sources will be false. It remains for the algorithm to be tested with different sources to determine the extent of this limitation. Additional computer simulations using the three dimensional bio-heat equation are also in order to further define the limitations of the algorithm. Most important are studies of the effects of the location of temperature sensors and of more complex geometries, especially situations in which extensive normal tissue intervenes between power applicators and tumor tissues.

Nevertheless, future implementation of control algorithms of this type, in conjunction with a multi-applicator hyperthermia systems, may lead both to a lower incidence of complications caused by hot spots within the treatment field and to a lower incidence of treatment failures caused by cold spots within the tumor.

REFERENCES

1. C. F. Babbs, D. P, DeWitt, W, D. Voorhees, J. S. McCaw, and R. C. Chan, "Theoretical feasibility of vasodilator enhanced local tumor heating," Euro. J. Cancer Clinical Oncol., vol. 18, no. 11, pp. 1137-1146, 1982.

2. R. C. Chan, C. F. Babbs, R. J. Vetter, and C. H. Lamar, "Abnormal response of tumor vasculature to vasoactive drugs," J. Natl. Cancer Institute, vol. 72, no. 1, pp. 145–150, 1984.

3. W. D, Voorhees and C. F. Babbs, "Hydralazine-enhanced selective heating of transmissible venereal tumor implants in dogs," Euro. J. Cancer Clinical Oncol., vol. 18, no. 10, pp. 1027-1034, 1982.

4. C. F. Babbs, J. R. Oleson, and J. A. Pearce, "Equipment for local hyperthermia therapy of cancer," Med. Instrument., vol. 16, pp. 245-248, 1982.

5. P. P. Lele and K. J. Parker, "Temperature distributions in tissues during local hyperthermia by stationary or steered beams of unfocused or focused ultrasound," Br. J. Cancer (Suppl. V), vol. 45, pp. 108-121, 1982.

6. M. R. Manning, T. C. Cetas, R. C. Miller, J. R. Oleson, W. G Connor, and E. W. Gemer, "Clinical hyperthermia: Results of a phase I trial employing hyperthermia alone or in combination with external beam or interstitial radiotherapy," Cancer, vol. 49, pp. 205-216, 1982.

7. C. F. Babbs, W. D. Voorhees, R. R. Clark, T. M. Skojac, and S. D. Meritt, "Use of combined systemic hypothermia and local heat treatment to enhance temperature differences between tumor and normal tissues," Med. Instrument., vol. 19, pp. 27–33, 1985.

8. J. W. Strohbehn and R. B. Roemer, "A survey of computer simulations of hyperthermia treatment," IEEE Trans. Biomed. Eng., vol. BME-31, pp. 136-149, 1984.

9. C. W. Song, M. S. Kang, J. G. Rhee, and S. H. Lewtt, "Effect of hyperthermia on vascular function in normal and neoplastic tissues," Ann. NY Acad. Sci., vol. 335, pp. 35-47, 1980.

10. C. W. Song, J. G. Rhee, and S. H. Levitt, "Blood flow in normal tissues and tumors during hyperthermia," J. Natl. Cancer Institute, vol. 64, pp. 119-124, 1980.

11. M. W. Dewhirst, D. A. Sire, S. Sapareto, and W. G. Connor, "Importance of minimum tumor temperature in determining early and long-term responses of spontaneous canine and feline tumors to heat and radiation," Cancer Res., vol. 44, pp. 43-50, 1984.